JACS
JOURNAL OF THE AMERICAN CHEMICAL SOCIETY

Article

Helical Sulfono-#-AApeptides with Aggregation-Induced Emission and Circularly Polarized Luminescence

Yan Shi, Guangqiang Yin, Zhiping Yan, Peng Sang, Minghui Wang, Robert Brzozowski, Prahathees Eswara, Lukasz Wojtas, You-Xuan Zheng, Xiaopeng Li, and Jianfeng Cai

J. Am. Chem. Soc., **Just Accepted Manuscript** • DOI: 10.1021/jacs.9b05329 • Publication Date (Web): 23 Jul 2019

Helical Sulfono-γ-AApeptides with Aggregation-Induced Emission and Circularly Polarized Luminescence

Yan Shi,[1,¶] Guangqiang Yin,[1,¶] Zhiping Yan,[3] Peng Sang,[1] Minghui Wang,[1] Robert Brzozowski,[2] Prahathees Eswara,[2] Lukasz Wojtas,[1] Youxuan Zheng,[3,*] Xiaopeng Li,[1,*] and Jianfeng Cai[1,*]

[1] Department of Chemistry, University of South Florida, 4202 East Fowler Avenue, Tampa, Florida 33620, United States.

[2] Department of Cell Biology, Microbiology and Molecular Biology, University of South Florida, 4202 East Fowler Avenue, Tampa, Florida 33620, United States.

[3] State Key Laboratory of Coordination Chemistry, School of Chemistry and Chemical Engineering, Nanjing University, 210023 Nanjing, China.

ABSTRACT: Aggregation-induced emission (AIE) was intensively studied owing to packing of small molecules and polymers, however, mid-molecular-weight (1000-3000) molecular scaffold containing precise number of AIE luminogens is rare. Herein we report the investigation of three tetraphenylethylene (TPE) modified sulfono-γ-AApeptides, in which multiple TPE moieties are conjugated to the chiral right-handed helical peptidomimetic backbone as functional side chains. The crystal structure of the TPE-α/sulfono-γ-AA peptide **1** demonstrates that due to the rigid helical scaffold of the TPE-α/sulfono-γ-AA peptides, the intramolecular rotations of the TPE with short linker are restricted, therefore leading to the boosted fluorescent emission in solution. Peptides **2** and **3** exhibit aggregation-induced emission enhancement (AIEE), possibly owing to combination of both AIE and rotation restriction. Moreover, due to their pre-oriented assembly induced by the right-handed helical scaffold, these emissive chiral luminogens show effective circularly polarized luminescence signals with high dissymmetry factor g_{lum}. Finally, the amphiphilic nature of TPE-α/ sulfono-γ-AA peptides could enable them to penetrate the bacterial membranes and exhibit strong fluorescence. Their antimicrobial activity and labeling-free character could further augment their potential applications in both materials and biomedical sciences.

Introduction

The development of aggregation-induced emission (AIE) materials has recently drawn considerable attention due to their applications in OLEDs, bioprobes, chemosensors, chiral recognition and so on.[1] Among the prototypical AIE luminogens (AIEgens), the tetraphenylethylene (TPE) derivatives are the most classic family and have been extensively explored. [2] In these emissive systems, the TPE derivatives were incorporated into the metal–organic frameworks (MOFs),[3] covalent organic frameworks (COFs),[4] metallo-macrocycles,[5] polymers,[6] and metallo-cages.[2b, 7] However, most of the designs are based on a same tactic, that is, the restriction of the intramolecular rotation (RIR) due to aggregation and packing of TPE moieties.[1f, 8] Upon aggregate formation, confinement of the rigid environment weakens the rotation of the four peripheral aromatic rotors against the central olefin stator in TPE, leading to the suppression of nonradiative decay pathways and the activation of the radiative decay in solid state.[1f] On this basis, lots of efforts have been made to restrict the rotation of the phenyl rings by covalent bond connection[1g] and coordination networks[9] so as to enhance fluorescence intensity. Instead of aggregation and packing, it is rare to turn on luminescent properties of TPEs at the single molecular level, e.g. in solution.[10]

In parallel to the intensive studies of AIE, circularly polarized luminescence (CPL) materials have also attracted increasing interests as circularly polarized light would improve the quality of the 3D image and decrease the damage to the eyes in display.[11] In the past years, the research investigation based on chiral luminescent systems has made significant progress, including metal complexes,[12] small organic luminophores,[13] conjugated polymers,[14] supramolecules,[15] and liquid crystals.[16] But except for the lanthanide complexes, most reported systems still suffered from the relatively low luminescence dissymmetry factor (g_{lum}) both in solution and solid state, ill-defined structure-property relationship, and chiroptical properties sensitive to the external environments. Therefore, it is still urgent to exploit material which could directly generate CPL,

particularly design and synthesis of a single molecule bearing CPL function rather than through the packing of molecules.

To tackle the challenges existing in both AIE and CPL, herein we report the properties of TPE modified 1:1 α/sulfono γ-AApeptides. The γ-AApeptide (oligomers of γ-substituted-*N*-acylated-*N*-aminoethyl amino acids) is a new class of the peptidomimetics, the backbone of which was inspired by the chiral PNA.[17] In the 1:1 α/sulfono-γ-AA peptides, the bulky sulfonamide groups induce a curvature conformation of the backbone, leading to the formation of robust right-handed 4_{13} windmill-shaped heliacal structures, which are confirmed by the crystal structure of homo/heterogeneous sulfono-γ-AA peptides as well as solution structures.[18,19] We hypothesized that when conjugated with the TPE moiety, the constrained helical backbone of the sulfono-γ-AA peptide would restrict the intramolecular rotation of the TPE, thereby inducing the fluorescence of these TPE conjugated sulfono- γ-AA peptides even at the single molecular level in solution. In addition, due to chiral arrangement/assembly of the TPE moieties induced by the right-handed helical sense of the molecular scaffold, these TPE-α/sulfono-γ-AA peptides would also be expected to exhibit good CPL properties, which are generated at single molecule level instead of intermolecular packing.

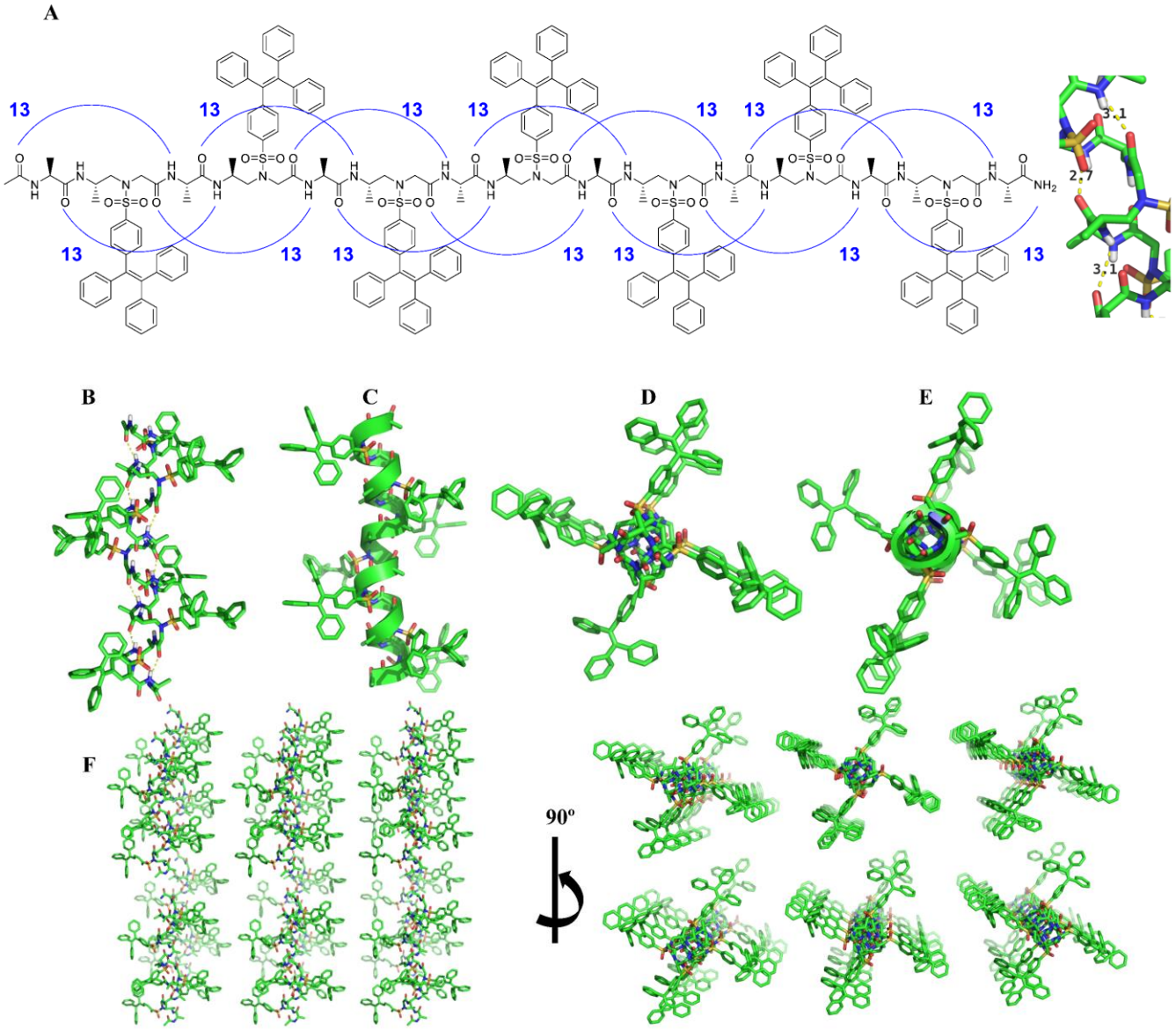

Figure 1. Chemical and crystal structure of TPE-α/sulfono-γ-AA peptide 1, the crystal structures are drwan by PyMol. A). Chemical structure and the 13-atom-hydrogen-bonding pattern. B). Crystal structure of the bonding pattern. C). Helical cartoon of the crystal structure. D). Crystal packing of 1 along the peptide axis. E). Cartoon structure of D. F). Packing mode of the crystal.

Results and Discussion

The first TPE-α/sulfono-γ-AA peptide **1** (Figure 1A) was designed by conjugation of TPEs directly onto the backbone of the 1:1 α/sulfono-γ-AA hybrid peptide. Particularly, TPE moieties were incorporated into sulfono-γ-AA building blocks and the TPE-conjugated 1:1 α/sulfono-γ-AA hybrid peptide **1** was obtained with decent yield by the solid-phase standard Fmoc chemistry based on our previous protocol.[17] The Crystal showed a 13-atom-hydrogen-bonding pattern, with 2.7 Å and 3.1 Å hydrogen-binding distance. The persistent and unified intramolecular H-bond network and organized packing of side chain unambiguously indicates that this class of oligomers, as a 4_{13} helix, could provide a particularly strong stabilization of this novel secondary structure motif (Figure 1A, S1). To our delight, TPE-α/sulfono-γ-AA peptide **1** was successfully solved by the single-crystal X-ray crystallography with resolutions of 1.5 Å. In the crystal structure, it shows that peptide **1** adopts right-handed helical conformation, with a diameter of 6.0 Å and pitch of 5.8 Å which are consistent to our previous reported related structures.[18a] There are exactly four side chains per helical turn, and TPE groups are present in a right-handed helical sense (Figure 1B-C). This led to a pseudo- four-fold symmetry of windmill-shape on the top view (Figure 1D-F).

On the basis of helical structures, we postulated that **1** could exhibit fluorescence at single molecular level even in solution because the seven TPE moieties are constrained on the helical scaffold. And such fluorescence enhancement is due to their rotation limitation rather than aggregation induced emission. To test our hypothesis, we next carried out absorption and fluorescence studies. As shown in Figure 2B, two strong peaks (250 nm and 350 nm) in the UV-vis spectrum of TPE-α/sulfono-γ-AA peptide **1** were observed as the typical absorption peaks of TPE moieties,[9] indicating that conjugation of TPE moieties to the helical peptide did not alter their intrinsic absorptive property. The result prompted us to move forward to study their potential fluorescent activity. The TPE-α/sulfono-γ-AA peptide **1** (Figure 2C) was found to be soluble in pure water, however, 99% PBS (Phosphate Buffered Saline) buffer is a poor solvent which led to the precipitation of **1** due to enhanced salt strength. It is very interesting that **1** exhibits strong fluorescence in pure water (Figure 2A), consistent to our postulation that helical molecular scaffold restricts the free rotation of TPE moieties, leading to significantly enhanced fluorescence even in solution. When the percentage of poor solvent PBS buffer fraction (f_{PBS}) is gradually increased from 0% to 99%, the fluorescence intensity shows no significant change (Figure 2A and 2D), with good quantum yield (Φ_F = 35%). It suggested that boosted fluorescence was due to restriction on TPE bond rotation instead of AIE.

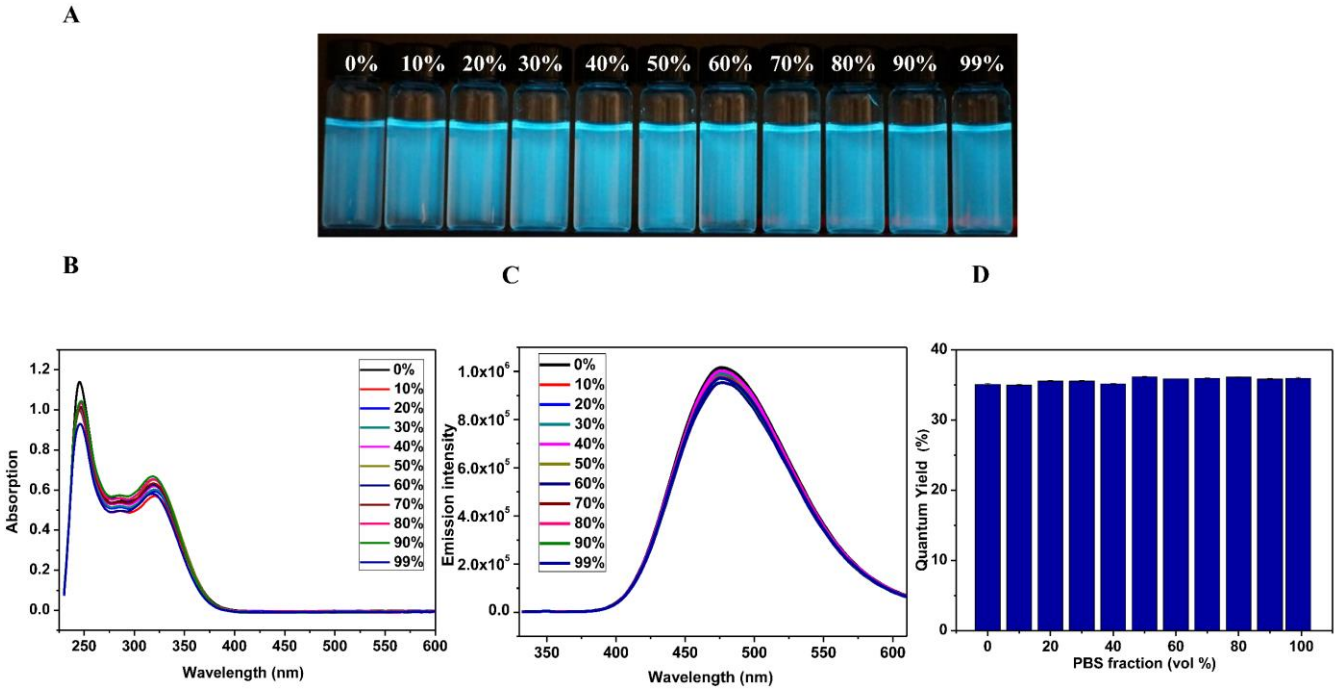

Figure 2. A). Photographs of **1** in water/PBS with various PBS fractions. B). UV/Vis spectra of **1** in water/PBS with various PBS fractions; C). Fluorescence spectra (λ_{ex} = 325 nm, c = 5.0 μM); D). Quantum yields.

To understand whether the stability of helical scaffold has impact on the fluorescent behavior of the TPE modified α/sulfono-γ-AA peptide, a new sequence **2** was also synthesized, in which the alanine residues in **1** was replaced with lysine residues (Figure 3A). Bearing amino side chains, **2** is expected to destabilize the helical scaffold due to the flexibility of side chains and electrostatic charge repulsion. Thus, we anticipated that the introduction of these amino side chains could confer TPE moieties with increased rotational freedom. Interestingly, although similar absorption and emission wavelengths were found in **2** (Figure 3B-D), **2** displayed different fluorescent behaviors compared to the

steady emission of **1** in both solutions and aggregation states. As shown in Figure 3E, the TPE-α/sulfono-γ-AApeptide **2** starts with a low Φ_F value (5%) in pure water, which may be due to the electrostatic repulsion of positively charge side chains that destabilize the helical scaffold. However, when the f_{PBS} increased from 0% to 10%, even though the sequence was still completely soluble, the charge repulsion could be shielded by PBS salts, which significantly enhanced the helical stability, leading to sharply increased Φ_F (35%). Further increase of PBS led to gradual aggregation of TPE-α/sulfono-γ-AApeptide **2** with enhanced quantum yield up to 45%. This is a typical AIE effect, by which aggregation further stabilized the helical structure and molecular packing, thereby enhancing fluorescence intensity.

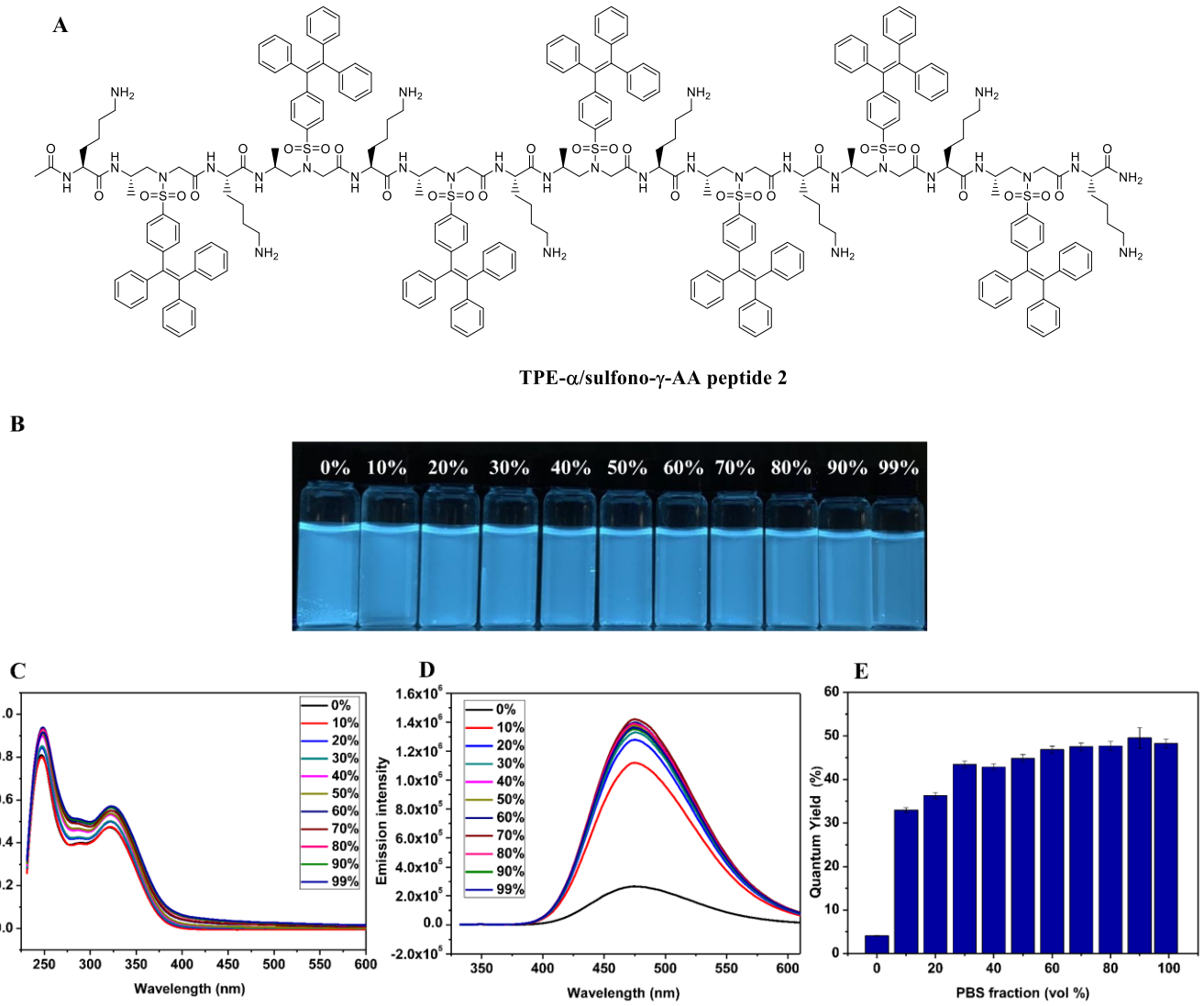

Figure 3. A). The structure of **2.** B). Photographs of **2** in water/PBS with various PBS fractions. C). UV/Vis spectra of **2** in water/PBS with various PBS fractions; D). Fluorescence spectra (λ_{ex} = 325 nm, c = 5.0 μM); E). Quantum yields.

After we explored the impact of helical scaffold on the fluorescence of TPE-α/sulfono-γ-AA peptides, we next asked if further induction of rotational freedom of TPE moieties could tune fluorescence behavior. As shown in Figure 4, a new sequence **3** was prepared. Unlike **1** and **2**, in which TPE moieties were conjugated to the backbone via sulfonyl group directly, the TPE moieties in the peptide **3** were attached by the amide bond via an additional flexible ethyl sulfonyl linker (Figure 4A). As anticipated, although helical molecular scaffold still gave fluorescence at 0% PBS (Φ_F = 20%), AIE took a more significant role than **2**, as seen for the Φ_F values at different f_w which demonstrated a gradual increment and reached the maximum (Φ_F = 79 %) at f_{PBS} = 60% (Figure 4E). We speculated that when TPE moieties were attached to the helical scaffold via a relatively longer and flexible linker, the restriction from the backbone became weaker, and as such the Φ_F was low when f_{PBS} was close to zero. It is worth noting that, as f_{PBS} increased, the fluorescence is boosted up through the combination of both helical scaffold stabilization as well as aggregation induced emission enhancement (AIEE).[20]

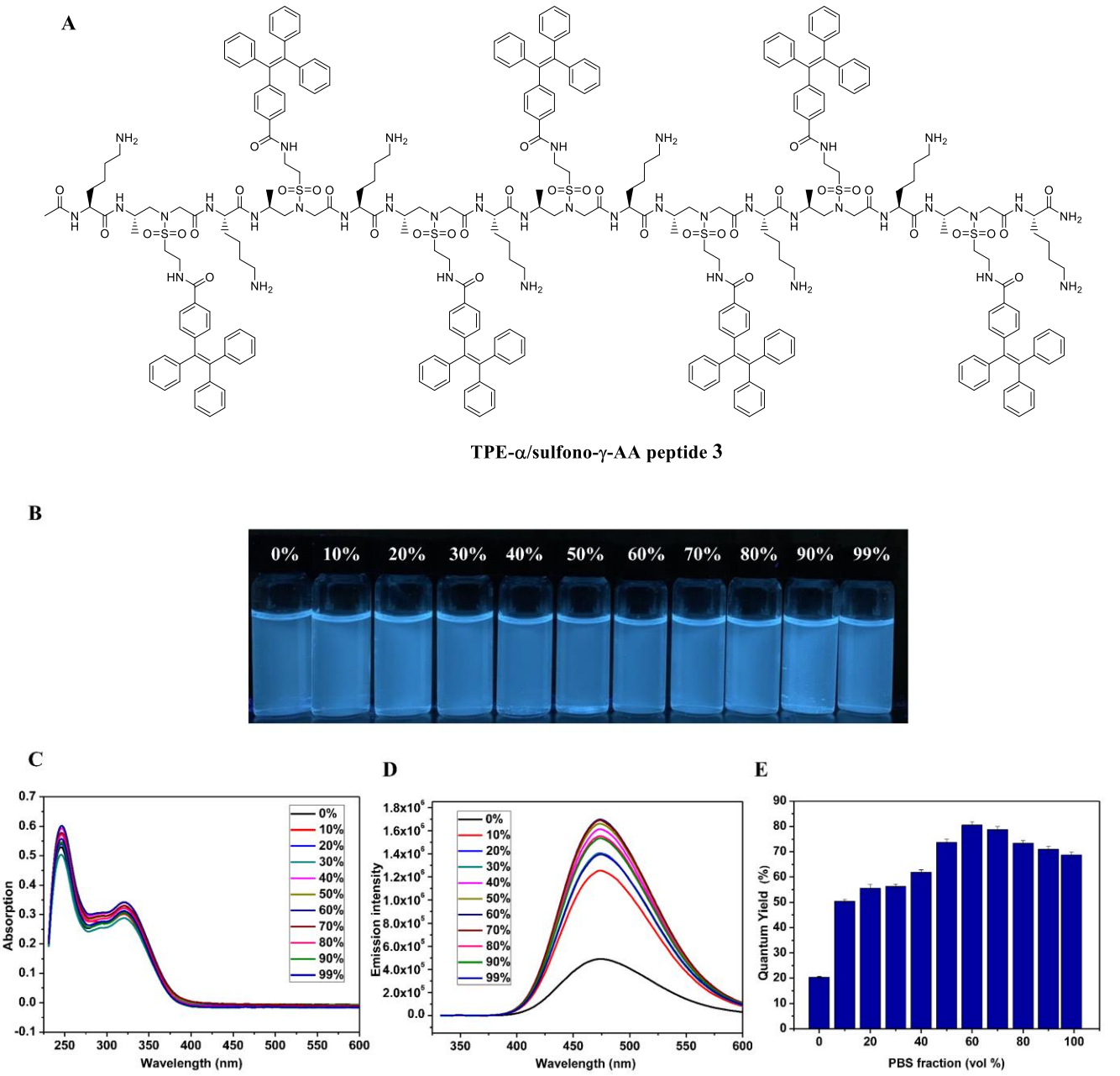

Figure 4. A). The structure of **3.** B). Photographs of **3** in water/PBS with various PBS fractions. C). UV/Vis spectra of **3** in water/PBS with various PBS fractions; D). Fluorescence spectra (λ_{ex} = 325 nm, c = 5.0 μM); E). Quantum yields.

To further investigate the emission properties of TPE-α/sulfono-γ-AA peptides **1-3**, we studied their aggregation behaviors by dynamic light scattering (DLS) and transmission electron microscopy (TEM). As shown in Figure 5, the TPE-α/sulfono-γ-AA peptides **1-3** were prone to forming nanosphere particles in solution. From the DLS results (Figure 5A-C), the average hydrodynamic diameters (Dh) of the TPE-α/sulfono-γ-AA peptides **1-3** nanospheres increased from 8.5, 5, 4 nm (0% PBS) to 15, 8, 7 nm (50% PBS), 18, 25, 8 nm (99% PBS). TEM was subsequently performed to further investigate the aggregation behavior of peptides. As shown in Figure 5D, the images of peptide **1** revealed that the size of these particles did not increase significantly with the Increment of PBS fraction, indicating that the helical structure took the predominant role in emission inducing, which was consistent with the result of the quantum yield. While for TPE-α/sulfono-γ-AA peptides **2** and **3** (Figure 5E, F), at 0% PBS in water, there is no obvious aggregated particle. But along with the increment of the PBS, the size and intensity of the particles became enlarged. These results are in good agreement with the observation that at higher percentage of PBS the emission was enhanced by the aggregation. Furthermore, at each PBS percentage of TPE-α/sulfono-γ-AA peptides **1-3**, the size of around 100 particles was measured by Image J, and the aggregate diameter distribution data was consistence with the DLS and TEM experiments (Figure S2).

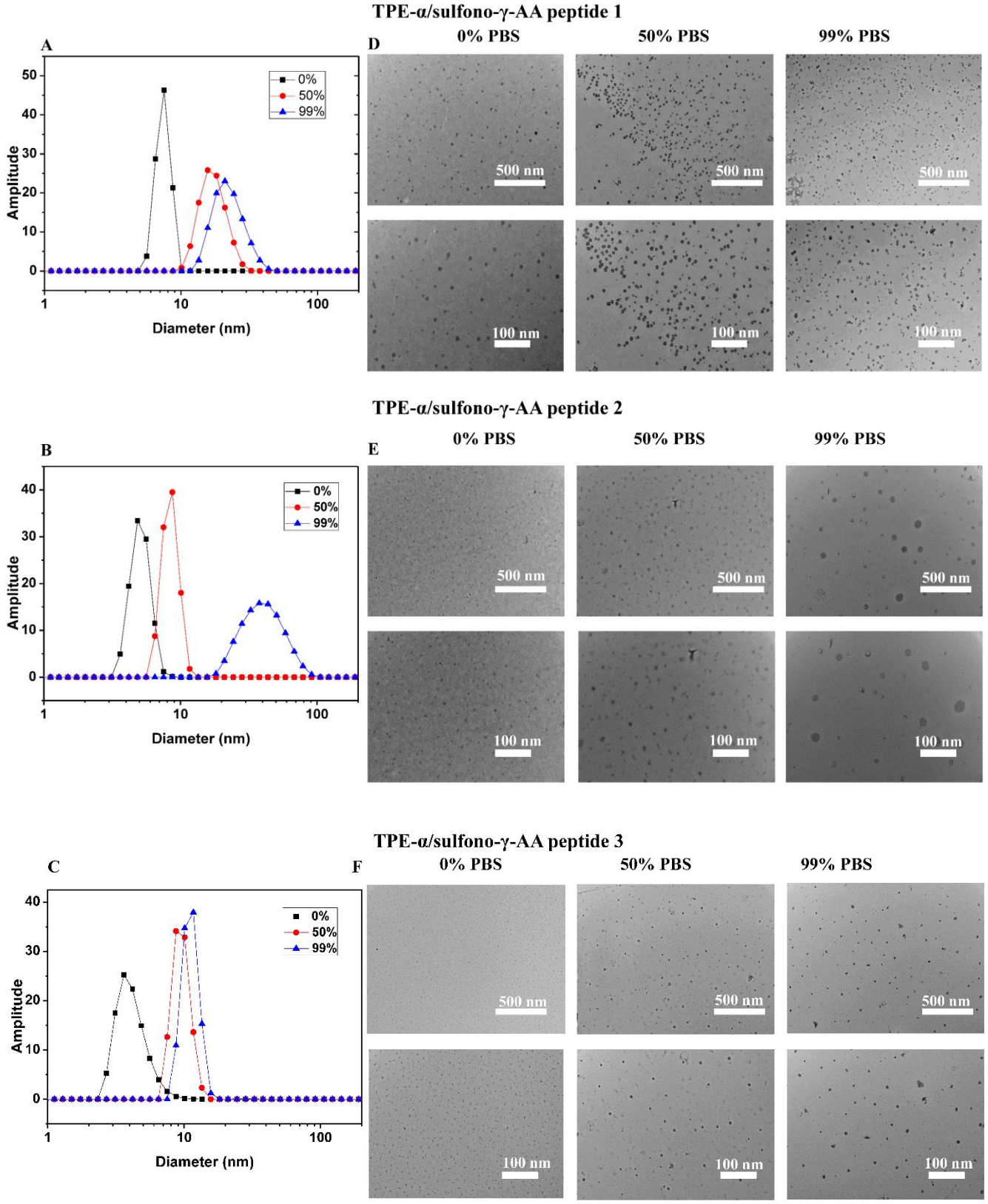

Figure 5. A-C DLS data and D-F TEM images of TPE-α/sulfono-γ-AA peptides **1-3** aggregates in 0% PBS, 50% PBS and 99% PBS (scale bar, 500 nm for D, E, F upper images and 100 nm for D, E, F, bottom images, respectively).

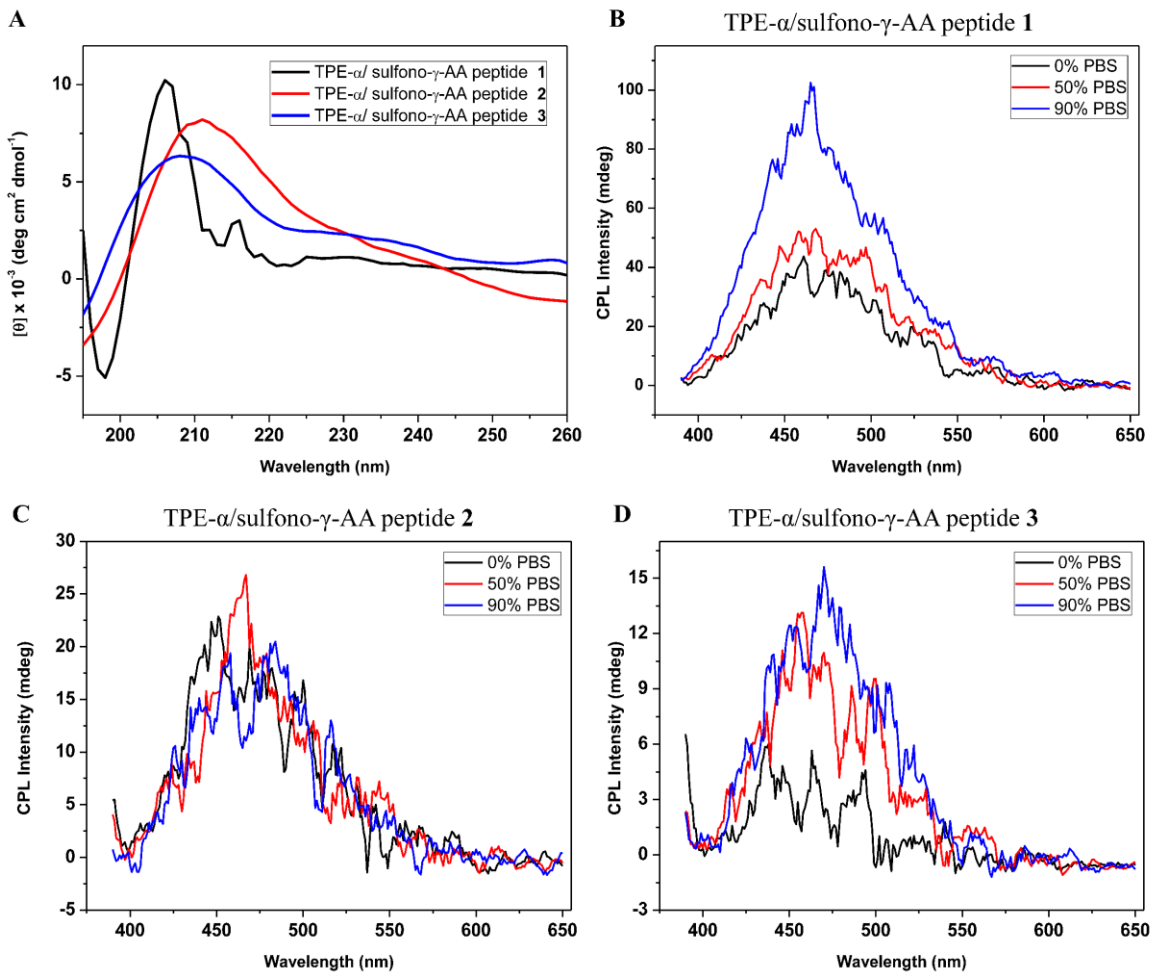

Figure 6. A). The CD spectra of the TPE-α/sulfono-γ-AA peptides **1-3** in H_2O/PBS 1:1. B-D). The CPL spectra of peptides **1-3** in PBS buffer percentage.

The circular dichroism (CD) spectra were next performed in H_2O/PBS (1:1) in the range of 195 - 260 nm in order to evaluate the helical propensity of the three peptides in solution. As shown in Figure 6A, all peptides show strong positive cotton effects between 205- 215 nm, suggesting that the TPE-α/sulfono-γ-AA peptides **1-3** adopt similar right-handed helical conformations.[18a] Interestingly, further CD study of peptide **2** at different solvent systems suggested that the sequence retained a good degree of helicity in the presence of water, while in other solvent system the cotton effect became relatively weaker (Figure S3).

Given the fact that these TPE moieties are arranged on the right-handed helical scaffold, and the chirality could be transferred from the chiral backbone of the γ-AApeptides, we envision that these luminous TPE-α/sulfono-γ-AA peptides would also generate CPL. To our delight, in the test of three sequences in different ratios of water/PBS buffer, intensive CPL signals were observed in all the samples. The highest calculated value of the dissymmetry factor (g_{lum}) is *ca.* 1.2 $\times 10^{-2}$, which is a large g_{lum} data compared with the reports ($\sim 10^{-5}$-10^{-3} order).[21] In the TPE-α/sulfono-γ-AA peptide **1**, the g_{lum} data is increasing accompanied by the increased PBS buffer percentage, while the g_{lum} data does not change dramatically of TPE-α/sulfono-γ-AA peptide **2-3** (Figure 6B-D). We speculate that these CPL helical foldamers are superior to known CPL small molecules and polymers, since polymers do not have defined structure whereas it is challenging to precisely control the packing of small chiral molecules.

The peptides **2** and **3** contains both cationic and hydrophobic groups, which satisfy the rationale for developing antimicrobial peptidomimetics mimicking host-defense peptides (HDPs): the cationic functional groups would bind to the negatively charged bacterial membranes, and the hydrophobic groups could subsequently lead to the disruption of the bacterial membranes.[22] Based on this assumption, we postulated that these two peptides would have antimicrobial activities. Indeed, **2** and **3** show IC_{50}s of 3.2 and 6.3 μg/mL in killing Gram-positive bacteria Methicillin-resistant *S. aureus* (*Staphylococcus aureus*, MRSA). MRSA is a significant opportunistic pathogen which is responsible for most hospital-acquired infection in the world.[23] As expected, peptide **1** did not show any antibacterial activity. Compounds bearing both fluorescence and bacteria-killing function could be developed for both diagnostic and antibiotics. Furthermore, as peptides **2** and **3** display strong

autofluorescence, we studied their localization and antibacterial activity through three dimensional, high-resolution, live-cell, fluorescence microscopy. Briefly, we treated the cells of Gram-positive *S. aureus* and *Bacillus subtilis* as well as Gram-negative *Escherichia coli* with the TPE-α/sulfono-γ-AA peptides **2** or **3** at the concentration of 0.05 mg/mL (1X), 0.25 mg/mL (5X), and 0.5 mg/mL (10X). Cells treated with the vehicle, dimethyl sulfoxide (DMSO), served as our negative control. As shown in Figure 7, *S. aureus* was sensitive to the treatment of peptides **2** or **3**, as indicated by the loss of cell shape, integrity, and lysis, at the concentrations of 5X and higher. At lower concentrations, the localization of both peptides around the cell periphery was evident, suggesting their antimicrobial property likely stems from membrane-binding. Similarly, peptides **2** and **3** appeared to localize to the cell membrane in *B. subtilis*, although cells were resistant to the peptide treatment as they were able to retain their cell shape and became sensitive only at 10X or higher concentrations. In *E. coli*, TPE-α/sulfono-γ-AA peptide **2** did not target to the cell surface and peptide **3** weakly associated with the cell periphery. *E. coli* cells were also resistant to peptide **2** treatment and were sensitive to peptide **3** only at higher concentrations. Thus, TPE-α/sulfono-γ-AA peptides **2** and **3** are potent anti-staphylococcal agents.

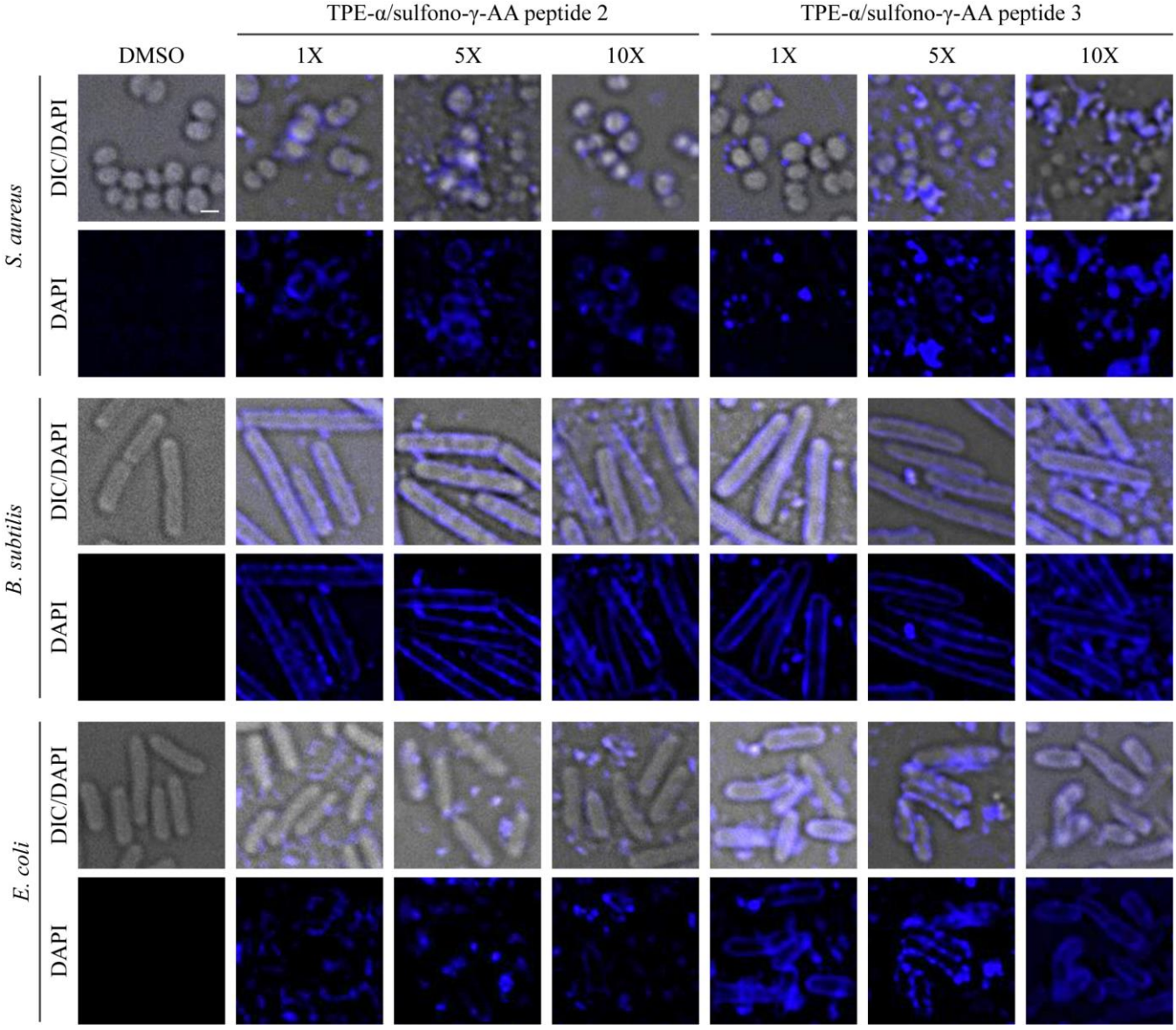

Figure 7. Micrographs of *S. aureus*, *B. subtilis*, and *E. coli* cells treated with 0.05 mg/mL (1X), 0.25 mg/mL (5X), and 0.5 mg/mL (10X) of TPE-α/sulfono-γ-AA peptides **2** or**3**. The vehicle for the peptides, DMSO, was used as a control. Differential interference contrast (DIC) and the autofluorescence of peptides obtained through standard DAPI filter are shown. Scale bar, 1 μm.

Conclusion

In this work, we designed and prepared a series of novel chiral and emissive TPE conjugated sulfono-γ-AApeptides. By investigating the structure and the properties, we identified that the helical peptide backbone provides a favorable scaffold to restrict the intramolecular rotations and induce fluorescence. The fluorescence could be synergistically enhanced by AIE effect. In addition, the right-handed helical framework could be used to precisely arrange the distribution of TPE moieties, which lead to the large CPL dissymmetric factor as high as 1.2×10^{-2}, augmenting their great potential in chiral recognition and enantioselective catalysis. The autofluorescence property could be adopted for the investigation of mechanism of antimicrobial action.

ASSOCIATED CONTENT

Supporting Information.

"This material is available free of charge via the Internet at http://pubs.acs.org."

Synthetic routes, characterization data, X-ray crystallographic data, HPLC traces, additional figures.

AUTHOR INFORMATION

Corresponding Author

* jianfengcai@usf.edu
xiaopengli1@usf.edu
yxzheng@nju.edu.cn

Author Contributions

¶ These authors contributed equally to this work.

Notes

The authors declare no conflict of interest.

ACKNOWLEDGMENT

The work was supported by NSF 1708500 (JC), NIH 1R01GM112652-01A1 (JC).

REFERENCES

1. (a) Shi, H.; Liu, J.; Geng, J.; Tang, B. Z.; Liu, B., Specific Detection of Integrin αvβ3 by Light-Up Bioprobe with Aggregation-Induced Emission Characteristics. *J. Am. Chem. Soc.***2012,** *134*, 9569-9572; (b) Wang, J.; Mei, J.; Hu, R.; Sun, J. Z.; Qin, A.; Tang, B. Z., Click Synthesis, Aggregation-Induced Emission, E/Z Isomerization, Self-Organization, and Multiple Chromisms of Pure Stereoisomers of a Tetraphenylethene-Cored Luminogen. *J. Am. Chem. Soc.***2012,** *134*, 9956-9966; (c) Wu, W.; Ye, S.; Huang, L.; Xiao, L.; Fu, Y.; Huang, Q.; Yu, G.; Liu, Y.; Qin, J.; Li, Q.; Li, Z., A conjugated hyperbranched polymer constructed from carbazole and tetraphenylethylene moieties: convenient synthesis through one-pot "A2 + B4" Suzuki polymerization, aggregation-induced enhanced emission, and application as explosive chemosensors and PLEDs. *J. Mater. Chem.* **2012,** *22*, 6374-6382; (d) Mei, J.; Hong, Y.; Lam, J. W. Y.; Qin, A.; Tang, Y.; Tang, B. Z., Aggregation-Induced Emission: The Whole Is More Brilliant than the Parts. *Adv. Mater.* **2014,** *26*, 5429-5479; (e) Yoshii, R.; Hirose, A.; Tanaka, K.; Chujo, Y., Functionalization of Boron Diiminates with Unique Optical Properties: Multicolor Tuning of Crystallization-Induced Emission and Introduction into the Main Chain of Conjugated Polymers. *J. Am. Chem. Soc.***2014,** *136*, 18131-18139; (f) Mei, J.; Leung, N. L. C.; Kwok, R. T. K.; Lam, J. W. Y.; Tang, B. Z., Aggregation-Induced Emission: Together We Shine, United We Soar! *Chem. Rev.* **2015,** *115*, 11718-11940; (g) Xiong, J.-B.; Feng, H.-T.; Sun, J.-P.; Xie, W.-Z.; Yang, D.; Liu, M.; Zheng, Y.-S., The Fixed Propeller-Like Conformation of Tetraphenylethylene that Reveals Aggregation-Induced Emission Effect, Chiral Recognition, and Enhanced Chiroptical Property. *J. Am. Chem. Soc.***2016,** *138*, 11469-11472; (h) Zheng, J.; Ye, T.; Chen, J.; Xu, L.; Ji, X.; Yang, C.; He, Z., Highly sensitive fluorescence detection of heparin based on aggregation-induced emission of a tetraphenylethene derivative. *Biosens. Bioelectron.* **2017,** *90*, 245-250.

2. (a) Hong, Y.; Lam, J. W. Y.; Tang, B. Z., Aggregation-induced emission: phenomenon, mechanism and applications. *Chem. Commun.* **2009**, 4332-4353; (b) Wang, M.; Zheng, Y.-R.; Ghosh, K.; Stang, P. J., Metallosupramolecular Tetragonal Prisms via Multicomponent Coordination-Driven Template-Free Self-Assembly. *J. Am. Chem. Soc.* **2010,** *132*, 6282-6283; (c) Hong, Y.; Lam, J. W. Y.; Tang, B. Z., Aggregation-induced emission. *Chem. Soc. Rev.* **2011,** *40*, 5361-5388; (d) Chi, Z.; Zhang, X.; Xu, B.; Zhou, X.; Ma, C.; Zhang, Y.; Liu, S.; Xu, J., Recent advances in organic mechanofluorochromic materials. *Chem. Soc. Rev.* **2012,** *41*, 3878-3896; (e) Ding, D.; Li, K.; Liu, B.; Tang, B. Z., Bioprobes Based on AIE Fluorogens. *Acc. Chem. Res.* **2013,** *46*, 2441-2453; (f) Kwok, R. T. K.; Leung, C. W. T.; Lam, J. W. Y.; Tang, B. Z., Biosensing by luminogens with aggregation-induced emission characteristics. *Chem. Soc. Rev.* **2015,** *44*, 4228-4238.

3. (a) Shustova, N. B.; McCarthy, B. D.; Dincă, M., Turn-On Fluorescence in Tetraphenylethylene-Based Metal–Organic Frameworks: An Alternative to Aggregation-Induced Emission. *J. Am. Chem. Soc.***2011,** *133*, 20126-20129; (b) Gong, Q.; Hu, Z.; Deibert, B. J.; Emge, T. J.; Teat, S. J.; Banerjee, D.; Mussman, B.; Rudd, N. D.; Li, J., Solution Processable MOF Yellow Phosphor with Exceptionally High Quantum Efficiency. *J. Am. Chem. Soc.***2014,** *136*, 16724-16727; (c) Zhang, M.; Feng, G.; Song, Z.; Zhou, Y.-P.; Chao, H.-Y.; Yuan, D.; Tan, T. T. Y.; Guo, Z.; Hu, Z.; Tang, B. Z.; Liu, B.; Zhao, D., Two-Dimensional Metal–Organic Framework with Wide Channels and Responsive Turn-On Fluorescence for the Chemical Sensing of Volatile Organic Compounds. *J. Am. Chem. Soc.***2014,** *136*, 7241-7244.

4. (a) Zhou, T.-Y.; Xu, S.-Q.; Wen, Q.; Pang, Z.-F.; Zhao, X., One-Step Construction of Two Different Kinds of Pores in a 2D Covalent Organic Framework. *J. Am. Chem. Soc.***2014,** *136*, 15885-15888; (b) Ascherl, L.; Sick, T.; Margraf, J. T.; Lapidus, S. H.; Calik, M.; Hettstedt, C.; Karaghiosoff, K.; Döblinger, M.; Clark, T.; Chapman, K. W.; Auras, F.; Bein, T., Molecular docking sites designed for the generation of highly crystalline covalent organic frameworks. *Nat. Chem.* **2016,** *8*, 310; (c) Dalapati, S.; Jin, E.; Addicoat, M.; Heine, T.; Jiang, D., Highly Emissive Covalent Organic Frameworks. *J. Am. Chem. Soc.* **2016,** *138*, 5797-5800.

5. (a) Chen, L.-J.; Ren, Y.-Y.; Wu, N.-W.; Sun, B.; Ma, J.-Q.; Zhang, L.; Tan, H.; Liu, M.; Li, X.; Yang, H.-B., Hierarchical Self-Assembly of Discrete Organoplatinum(II) Metallacycles with Polysaccharide via Electrostatic Interactions and Their Application for Heparin Detection. *J. Am. Chem. Soc.* **2015,** *137*, 11725-11735; (b) Yan, X.; Wang, H.; Hauke, C. E.; Cook, T. R.; Wang, M.; Saha, M. L.; Zhou, Z.; Zhang, M.; Li, X.; Huang, F.; Stang, P. J., A Suite of Tetraphenylethylene-Based Discrete Organoplatinum(II) Metallacycles: Controllable Structure and Stoichiometry, Aggregation-Induced Emission, and Nitroaromatics Sensing. *J. Am. Chem. Soc.* **2015,** *137*, 15276-15286; (c) Yan, X.; Wang, M.; Cook, T. R.; Zhang, M.; Saha, M. L.; Zhou, Z.; Li, X.; Huang, F.; Stang, P. J., Light-Emitting Superstructures with Anion Effect: Coordination-Driven Self-Assembly of Pure Tetraphenylethylene Metallacycles and Metallacages. *J. Am. Chem. Soc.* **2016,** *138*, 4580-4588; (d) Zhou, Z.; Yan, X.; Saha, M. L.; Zhang, M.; Wang, M.; Li, X.; Stang, P. J., Immobilizing Tetraphenylethylene into Fused Metallacycles:

Shape Effects on Fluorescence Emission. *J. Am. Chem. Soc.* **2016,** *138*, 13131-13134.
6. (a) Lu, C.; Zhang, M.; Tang, D.; Yan, X.; Zhang, Z.; Zhou, Z.; Song, B.; Wang, H.; Li, X.; Yin, S.; Sepehrpour, H.; Stang, P. J., Fluorescent Metallacage-Core Supramolecular Polymer Gel Formed by Orthogonal Metal Coordination and Host–Guest Interactions. *J. Am. Chem. Soc.* **2018,** *140*, 7674-7680; (b) Peng, H.-Q.; Zheng, X.; Han, T.; Kwok, R. T. K.; Lam, J. W. Y.; Huang, X.; Tang, B. Z., Dramatic Differences in Aggregation-Induced Emission and Supramolecular Polymerizability of Tetraphenylethene-Based Stereoisomers. *J. Am. Chem. Soc.* **2017,** *139*, 10150-10156; (c) Xu, Y.; Chen, L.; Guo, Z.; Nagai, A.; Jiang, D., Light-Emitting Conjugated Polymers with Microporous Network Architecture: Interweaving Scaffold Promotes Electronic Conjugation, Facilitates Exciton Migration, and Improves Luminescence. *J. Am. Chem. Soc.* **2011,** *133*, 17622-17625.
7. (a) Yan, X.; Cook, T. R.; Wang, P.; Huang, F.; Stang, P. J., Highly emissive platinum(II) metallacages. *Nat. Chem.* **2015,** *7*, 342; (b) Givelet, C. C.; Dron, P. I.; Wen, J.; Magnera, T. F.; Zamadar, M.; Čépe, K.; Fujiwara, H.; Shi, Y.; Tuchband, M. R.; Clark, N.; Zbořil, R.; Michl, J., Challenges in the Structure Determination of Self-Assembled Metallacages: What Do Cage Cavities Contain, Internal Vapor Bubbles or Solvent and/or Counterions? *J. Am. Chem. Soc.* **2016,** *138*, 6676-6687; (c) Yu, G.; Cook, T. R.; Li, Y.; Yan, X.; Wu, D.; Shao, L.; Shen, J.; Tang, G.; Huang, F.; Chen, X.; Stang, P. J., Tetraphenylethene-based highly emissive metallacage as a component of theranostic supramolecular nanoparticles. *Proc. Natl Acad. Sci. USA* **2016,** *113*, 13720; (d) Zhang, M.; Saha, M. L.; Wang, M.; Zhou, Z.; Song, B.; Lu, C.; Yan, X.; Li, X.; Huang, F.; Yin, S.; Stang, P. J., Multicomponent Platinum(II) Cages with Tunable Emission and Amino Acid Sensing. *J. Am. Chem. Soc.* **2017,** *139*, 5067-5074.
8. Hu, R.; Leung, N. L. C.; Tang, B. Z., AIE macromolecules: syntheses, structures and functionalities. *Chem. Soc. Rev.* **2014,** *43*, 4494-4562.
9. Yin, G. Q.; Wang, H.; Wang, X. Q.; Song, B.; Chen, L. J.; Wang, L.; Hao, X. Q.; Yang, H. B.; Li, X., Self-assembly of emissive supramolecular rosettes with increasing complexity using multitopic terpyridine ligands. *Nat. Commun.* **2018,** *9*, 567.
10. Morishima, K.; Ishiwari, F.; Matsumura, S.; Fukushima, T.; Shibayama, M., Mesoscopic Structural Aspects of Ca2+-Triggered Polymer Chain Folding of a Tetraphenylethene-Appended Poly(acrylic acid) in Relation to Its Aggregation-Induced Emission Behavior. *Macromolecules* **2017,** *50* , 5940-5945.
11. (a) Han, J.; Guo, S.; Lu, H.; Liu, S.; Zhao, Q.; Huang, W., Recent Progress on Circularly Polarized Luminescent Materials for Organic Optoelectronic Devices. *Adv. Opt. Mater.***2018,** *6*, 1800538. (b) Huang, G.; Wen, R.; Wang, Z.; Li, B. S.; Tang, B. Z., Novel chiral aggregation induced emission molecules: self-assembly, circularly polarized luminescence and copper(ii) ion detection. *Mater. Chem. Front.* **2018,** *2*, 1884-1892. (c) Song, F.; Xu, Z.; Zhang, Q.; Zhao, Z.; Zhang, H.; Zhao, W.; Qiu, Z.; Qi, C.; Zhang, H.; Sung, H. H. Y.; Williams, I. D.; Lam, J. W. Y.; Zhao, Z.; Qin, A.; Ma, D.; Tang, B. Z., Highly Efficient Circularly Polarized Electroluminescence from Aggregation-Induced Emission Luminogens with Amplified Chirality and Delayed Fluorescence. *Adv. Funct. Mater.* **2018,** *28*, 1800051.
12. (a) Morita, M.; Rau, D.; Herren, M., Circularly polarized luminescence and enantiomeric energy transfer discrimination of chiral Tb(III)–Nd(III) EDDS and related complexes. *J. Alloys Compd* **2004,** *380*, 260-267; (b) Do, K.; Muller, F. C.; Muller, G., A Promising Change in the Selection of the Circular Polarization Excitation Used in the Measurement of Eu(III) Circularly Polarized Luminescence. *J. Phys. Chem. A* **2008,** *112*, 6789-6793; (c) Zinna, F.; Giovanella, U.; Bari, L. D., Highly Circularly Polarized Electroluminescence from a Chiral Europium Complex. *Adv. Mater.* **2015,** *27*, 1791-1795.
13. (a) Feuillastre, S.; Pauton, M.; Gao, L.; Desmarchelier, A.; Riives, A. J.; Prim, D.; Tondelier, D.; Geffroy, B.; Muller, G.; Clavier, G.; Pieters, G., Design and Synthesis of New Circularly Polarized Thermally Activated Delayed Fluorescence Emitters. *J. Am. Chem. Soc.* **2016,** *138*, 3990-3993; (b) Cerdán, L.; Moreno, F.; Johnson, M.; Muller, G.; de la Moya, S.; García-Moreno, I., Circularly polarized laser emission in optically active organic dye solutions. *Phys. Chem. Chem. Phys.* **2017,** *19*, 22088-22093; (c) He, D.-Q.; Lu, H.-Y.; Li, M.; Chen, C.-F., Intense blue circularly polarized luminescence from helical aromatic esters. *Chem. Commun.* **2017,** *53*, 6093-6096.
14. (a) Geng, Y.; Trajkovska, A.; Katsis, D.; Ou, J. J.; Culligan, S. W.; Chen, S. H., Synthesis, Characterization, and Optical Properties of Monodisperse Chiral Oligofluorenes. *J. Am. Chem. Soc.* **2002,** *124*, 8337-8347; (b) Watanabe, K.; Sakamoto, T.; Taguchi, M.; Fujiki, M.; Nakano, T., A chiral π-stacked vinyl polymer emitting white circularly polarized light. *Chem. Commun.* **2011,** *47*, 10996-10998; (c) Zheng, C.; An, Z.; Nakai, Y.; Tsuboi, T.; Wang, Y.; Shi, H.; Chen, R.; Li, H.; Ji, Y.; Li, J.; Huang, W., Relationships between main-chain chirality and photophysical properties in chiral conjugated polymers. *J. Mater. Chem. C* **2014,** *2*, 7336-7347.
15. (a) Goto, T.; Okazaki, Y.; Ueki, M.; Kuwahara, Y.; Takafuji, M.; Oda, R.; Ihara, H., Induction of Strong and Tunable Circularly Polarized Luminescence of Nonchiral, Nonmetal, Low-Molecular-Weight Fluorophores Using Chiral Nanotemplates. *Angew. Chem. Int. Ed.* **2017,** *56*, 2989-2993; (b) Han, J.; You, J.; Li, X.; Duan, P.; Liu, M., Full-Color Tunable Circularly Polarized Luminescent Nanoassemblies of Achiral AIEgens in Confined Chiral Nanotubes. *Adv. Mater.* **2017,** *29*, 1606503; (c) Shang, X.; Song, I.; Ohtsu, H.; Lee, Y. H.; Zhao, T.; Kojima, T.; Jung, J. H.; Kawano, M.; Oh, J. H., Supramolecular Nanostructures of Chiral Perylene Diimides with Amplified Chirality for High-Performance Chiroptical Sensing. *Adv. Mater.* **2017,** *29*, 1605828; (d) Wang, Y.; Li, X.; Li, F.; Sun, W.-Y.; Zhu, C.; Cheng, Y., Strong circularly polarized luminescence induced from chiral supramolecular assembly of helical nanorods. *Chem. Commun.* **2017,** *53*, 7505-7508.
16. (a) Chen, S. H.; Katsis, D.; Schmid, A. W.; Mastrangelo, J. C.; Tsutsui, T.; Blanton, T. N., Circularly polarized light generated by photoexcitation of luminophores in glassy liquid-crystal films. *Nature* **1999,** *397*, 506; (b) Katsis, D.; Kim, D. U.; Chen, H. P.; othberg, L. J.; Chen, S. H.; Tsutsui, T., Circularly Polarized Photoluminescence from Gradient-Pitch Chiral-Nematic Films. *Chem. Mater.* **2001,** *13*, 643-647.
17. Shi, Y.; Teng, P.; Sang, P.; She, F.; Wei, L.; Cai, J., γ-AApeptides: Design, Structure, and Applications. *Acc. Chem. Res.* **2016,** *49*, 428-441.
18. (a) Teng, P.; Ma, N.; Cerrato, D. C.; She, F.; Odom, T.; Wang, X.; Ming, L. J.; van der Vaart, A.; Wojtas, L.; Xu, H.; Cai, J., Right-Handed Helical Foldamers Consisting of De Novo d-AApeptides. *J. Am. Chem. Soc.* **2017,** *139*, 7363-7369; (b) She, F.; Teng, P.; Peguero-Tejada, A.; Wang, M.; Ma, N.; Odom, T.; Zhou, M.; Gjonaj, E.; Wojtas, L.; van der Vaart, A.; Cai, J., De Novo Left-Handed Synthetic Peptidomimetic Foldamers. *Angew. Chem. Int. Ed.* **2018,** *57*, 9916-9920.
19. (a) Teng, P.; Niu, Z.; She, F.; Zhou, M.; Sang, P.; Gray, G. M.; Verma, G.; Wojtas, L.; van der Vaart, A.; Ma, S.; Cai, J., Hydrogen-Bonding-Driven 3D Supramolecular Assembly of Peptidomimetic Zipper. *J. Am. Chem. Soc.* **2018,** *140*, 5661-5665; (b) Wu, H.; Qiao, Q.; Teng, P.; Hu, Y.; Antoniadis, D.; Zuo, X.; Cai, J., New Class of Heterogeneous Helical Peptidomimetics. *Org. Lett.* **2015,** *17*, 3524-3527.
20. (a) Wang, D.; Li, S.-M.; Zheng, J.-Q.; Kong, D.-Y.; Zheng, X.-J.; Fang, D.-C.; Jin, L.-P., Coordination-Directed Stacking and Aggregation-Induced Emission Enhancement of the Zn(II) Schiff Base Complex. *Inorg. Chem.* **2017,** *56*, 984-990; (b) Tang, W.; Xiang, Y.; Tong, A., Salicylaldehyde Azines as Fluorophores of Aggregation-Induced Emission Enhancement Characteristics. *J. Org. Chem.***2009,** *74*, 2163-2166; (c) Lamère, J.-F.; Saffon, N.; Dos Santos, I.; Fery-Forgues, S., Aggregation-Induced Emission Enhancement in Organic Ion Pairs. *Langmuir* **2010,** *26*, 10210-10217; (d) Feng, X.; Tong, B.; Shen, J.; Shi, J.; Han, T.; Chen, L.; Zhi, J.; Lu, P.; Ma, Y.; Dong, Y., Aggregation-Induced Emission Enhancement of Aryl-Substituted Pyrrole Derivatives. *J. Phys. Chem. B* **2010,** *114*, 16731-16736.

21. Yang, D.; Duan, P.; Zhang, L.; Liu, M., Chirality and energy transfer amplified circularly polarized luminescence in composite nanohelix. *Nat. Commun.* **2017,** *8*, 15727.
22. Li, Y.; Wu, H.; Teng, P.; Bai, G.; Lin, X.; Zuo, X.; Cao, C.; Cai, J., Helical Antimicrobial Sulfono-γ-AApeptides. *J. Med. Chem.* **2015,** *58*, 4802-4811.
23. Niu, Y.; Padhee, S.; Wu, H.; Bai, G.; Qiao, Q.; Hu, Y.; Harrington, L.; Burda, W. N.; Shaw, L. N.; Cao, C.; Cai, J., Lipo-γ-AApeptides as a New Class of Potent and Broad-Spectrum Antimicrobial Agents. *J. Med. Chem.* **2012,** *55*, 4003-4009.

Table of Contents artwork